ISSN 1063-7745, Crystallography Reports, 2017, Vol. 62, No. 6, pp. 868–880. © Pleiades Publishing, Inc., 2017.

STRUCTURE OF ORGANIC COMPOUNDS

N-[4-(3-Methyl-3-phenyl-cyclobutyl)-thiazol-2-yl]-*N*'-pyridin-2-ylmethylene-chloro-acetic Acid Hydrazide: Synthesis and Configurational Assignment Based on X-ray, ^{1}H, and ^{13}C NMR and Theoretical Calculations[1]

Sibel Demir[a,*], Muharrem Dinçer[b], Alaaddin Çukurovali[c], and Ibrahim Yılmaz[d]

[a] *Technical Science Vocational High School, Gaziantep University, Gaziantep, 27310 Turkey*

[b] *Department of Physics, Faculty of Arts and Sciences, Ondokuz Mayıs University, Kurupelit, Samsun, 55139 Turkey*

[c] *Department of Chemistry, Faculty of Science, Firat University, Elazığ, 23119 Turkey*

[d] *Department of Chemistry, Faculty of Science, University of Karamanoğlu Mehmet Bey, Karaman, 70200 Turkey*

**e-mail: sibeld@gantep.edu.tr*

Received January 13, 2016

Abstract—In this study, quantum chemical calculations based on the density functional theory have been carried out to examine the effects of *N*-[4-(3-methyl-3-phenyl-cyclobutyl)-thiazol-2-yl]-*N*'-pyridin-2-ylmethylene-chloro-acetic acid hydrazide. The calculated values are compared with the experimental data available for these molecules as a mean of validation of our proposed chemistry model. Aided by normal coordinate analysis and potential energy distributions, a confident vibrational assignment of all fundamentals is proposed herein. Additional support is given by ^{1}H and ^{13}C NMR spectra recorded with the sample dissolved in $CDCl_3$ and by predicted chemical shifts at the B3LYP/6-31G(*d*)/6-311G+(*d*) levels obtained using the gauge-invariant atomic orbital method. The calculated HOMO and LUMO energies also confirm that the charge transfer occurs within the molecule. Thiazole-based compounds are potential storehouse for exploiting CH···O and CH···N hydrogen bonding interactions for molecular self-assembly.

DOI: 10.1134/S1063774517060086

INTRODUCTION

Molecular modeling is a method which combines computational chemistry techniques with graphics visualization for simulating and predicting the three-dimensional structure, chemical processes and physicochemical properties of molecules and solids [1]. We understand for model chemistry (or theoretical model chemistry), the implementation of a theoretical model which should be uniformly applicable to molecular systems of any size and type up to a maximum size determined only by the practical availability of computer resources. This can be accomplished by linking a density functional for exchange and correlation with a particular basis set [2].

Thiazoles represent a very interesting class of compounds due to their wide applications in pharmaceutical, phytosanitary, analytical and industrial aspects, e.g., as antibacterial [3], fungicide [4, 5], anti-inflammatory [6–8], anthelmintics, antitubercular [9, 10], anti-HIV [11], antidegenerative [12] and hypothermic [13] activities, and herbicides [14] and have biological activities [15–20]. In recent years, thiazole-based chemosensors have also been investigated and shown to be successfully applicable in biological systems [21–25].

It is known that 2-aminothiazole is a biologically active compound with a broad range of activity and also it is an intermediate in the synthesis of antibiotics and dyes. Numerous thiazole derivative Schiff bases and their transition metal complexes have been investigated by various techniques [26–33].

The objective of this work is to perform a detailed calculation of the molecular structure of the *N*-[4-(3-methyl-3-phenyl-cyclobutyl)-thiazol-2-yl]-*N*'-pyridin-2-ylmethylene-chloro-acetic acid hydrazide (NNP2CH), as well as to predict their infrared (IR), and nuclear magnetic resonance (NMR), by using a new model chemistry within density functional theory (DFT) [34] and Hartree-Fock (HF), and to validate the calculated results by comparison with the experimental data available for these molecules as well as with the results of other theoretical models. Beginning

[1] The article is published in the original.

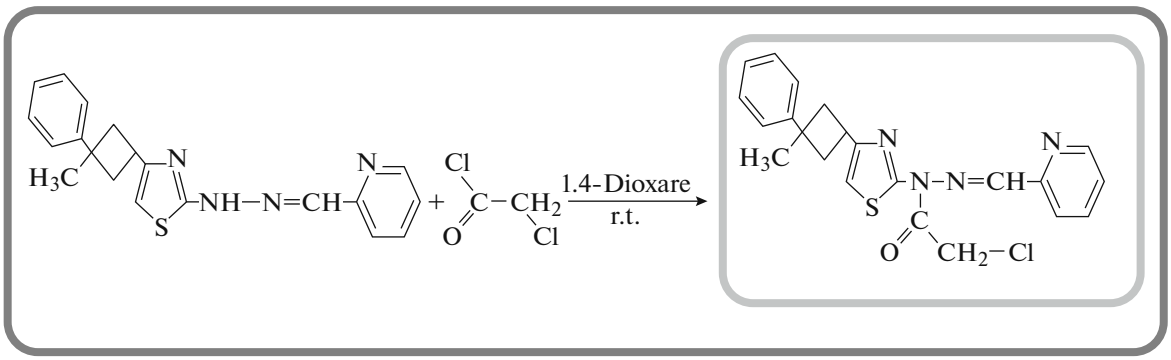

Fig. 1. Reaction sequence of synthesis of the title compound.

Table 1. Crystallographic characteristics and the X-ray data collection and structure-refinement parameters for the title compound

Formula	C_{23} H_{22} Cl N_3 O S
Formula weight	424.94
T, K	296
Wavelength, λ, Å	0.71073
Crystal system	Monoclinic
Sp. gr., Z	$P2_1/c$, 4
a, Å	8.1194(7)
b, Å	25.4054(12)
c, Å	11.1315(8)
β, deg	108.568(6)
V, Å^3	2176.6 (3)
D_{calc}, g cm^{-3}	1.260
F(000)	888
h, k, l ranges	$-10 \le h \le 8$ $-32 \le k \le 32$ $-14 \le l \le 14$
Reflections measured	12950
Reflections unique	4608
R_{int}	0.029
Reflections with $[I > 2\sigma(I)]$	2503
R_1 $[I > 2\sigma(I)]^a$	0.037
wR_2 $[I > 2\sigma(I)]^b$	0.094
S	0.83
Structure determination	SHELXS-97
Refinement	Full matrix
$\Delta\rho_{max}/\Delta\rho_{min}$, e/Å^3	0.14/−0.22

$^a R_1 = \Sigma\|F_o| - |F_c\|/\Sigma|F_o|$; $^b wR_2 = [\Sigma w(F_o^2 - F_c^2)^2/\Sigma w(F_o^2)^2]^{1/2}$.

model of the molecular structure is indicated in synthesis schema (Fig. 1).

EXPERIMENTAL

General Method

^{1}H and ^{13}C NMR spectra were recorded on a Bruker Avance III 400 spectrometer. Chemical shifts are reported on δ scale relative to TMS. Fourier-transform infrared (FT-IR) spectra were measured by an ATI Unicam-Mattson 1000 FT-IR spectrometer in the frequency range of 4000–400 cm^{-1} using KBr discs. CCDC 775740 contains the supplementary crystallographic data. The data can be obtained free of charge via http://www.ccdc.cam.ac.uk/conts/retrieving.html or from the Cambridge Crystallographic Data Centre, 12 Union Road, Cambridge CB2 1EZ, UK; fax: (+44) 1223-336-033; or e-mail: deposit@ccdc.cam.ac.uk.

Crystal Structure Determination and Refinements

X-ray data collection was carried out using a X-AREA diffractometer with a graphite monochromatized MoK_α radiation. Cell refinement: X-AREA; Data reduction: X-RED32 [35]; Program used to solve structure: SHELXS-97; Program(s) used to refine structure: SHELXL-97 [36]; Molecular graphics: ORTEP-3 for Windows [37].

X-ray diffraction study of NNP2CH ($C_{23}H_{22}ClN_3OS$) has been carried out and the data obtained are presented in Table 1. Diffraction intensities for NNP2CH were collected at 296 K on a Bruker Smart Apex (CCD) diffractometer (MoK_α, λ = 0.71073 Å). The organic hydrogen atoms were generated in ideal positions. Anisotropic thermal parameters were applied to all non-hydrogen atoms. A summary of key crystallographic information is given in Table 1.

Synthesis

The synthesis of the title compound was simply carried out in the following reaction scheme. A solution of 0.3485 g (1 mmol) of *N*-pyridin-2-ylmethylene-*N*'-[4-(3-methyl-3-phenyl-cyclobutyl)-thiazol-2-yl]-hydrazine was dissolved in 20 mL of dioxane containing triethylamine (1 mmol). To this solution, 90 μL (1 mmol) of chloroacetyl chloride solution in 20 mL 1,4-dioxane was added dropwise for two hours with stirring at room temperature. The mixture was stirred for two hours more and then neutralized with 5% aqueous ammonia (if necessary, but generally it is necessary). The compound precipitated was filtered, washed with copious water and crystallized from ethanol.

Pale yellow crystals: yield: 71%; m.p.: 111°C (EtOH); IR (KBr, ν cm^{-1}): 3102 (–NH–), 2986–2865 (aliphatics), 1716 (C=O), 1580 (C=N thiazole), 738 (>C–Cl), 628 (C–S); ^{1}H NMR ($CDCl_3$, TMS, δ ppm): 1.57 (s, 3H, $-CH_3$), 2.54 – 2.63 (m, 4H, $-CH_2-$ in cyclobutane ring), 3.84 (quint, j = 8.8 Hz, 1H, >CH– in cyclobutane ring), 4.84 (s, 2H, $-CH_2-$Cl), 7.04 (s, 1H, = CH–S in thiazole ring), 7.12–7.19 (m, 3H, aromatics), 7.26 – 7.34 (m, 3H, aromatics), 7.74 – 7.78 (m, 1H, aromatics), 7.94 (d, j = 7.7 Hz, 1H, aromatics), 8.35 (s, 1H, –N=CH–), 8.60 – 8.62 (m, 1H, aromatics); ^{13}C NMR ($CDCl_3$, TMS, δ ppm): 167.89, 158.89, 154.13, 152.92, 152.15, 149.91, 148.13, 136.89, 128.45, 125.58, 124.95, 120.97, 114.53, 43.41, 41.00, 39.16, 31.17, 30.16; anal. calc. for $C_{22}H_{21}ClN_4OS$ (424.95): C, 62.18; H, 4.98; N, 13.18; S, 7.55; found: C, 62.21; H, 5.03; N, 13.34; S, 7.89.

Computational Details

The molecular structure of this compound in the ground state was optimized by Becke 3–Lee–Yang–Parr (B3LYP) functional and by combining the results of the GaussView program [38]. Finally, the calculated normal mode vibrational frequencies and NMR were also calculated with these methods.

In order to obtain stable structures, the geometrical parameters in the ground state (in vacuo) were fully optimized at B3LYP levels of theory using the 6-31G(*d*) and 6-311G+(*d*) basis sets. The optimized structural parameters were used in the vibrational frequency calculations at B3LYP levels to characterize all stationary points as minima. Then vibrationally averaged nuclear positions of this compound were used for harmonic vibrational frequency calculations resulting in IR frequency together with intensities. Vibrational frequencies for these species were calculated using these methods and then scaled by 0.9613 [38, 39] and 0.9680 [39] for B3LYP/6-31G(*d*) and 6-311G+(*d*), respectively. The vibrational band's assignments have been made by using both the animation option of GaussView 3.0 graphical interface for Gaussian program [40].

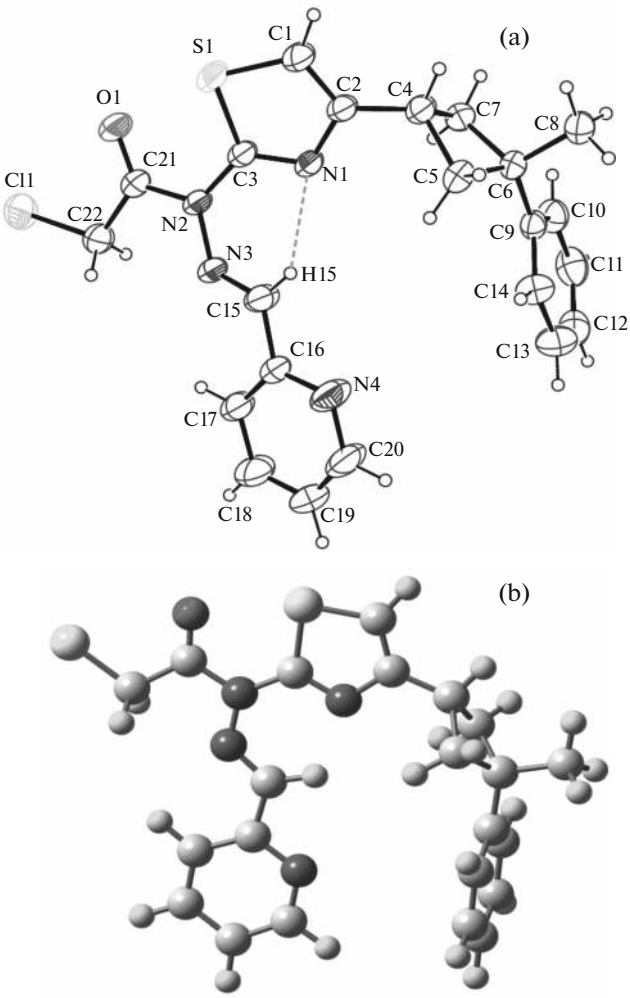

Fig. 2. ORTEP-3 drawing of the title compound with the atom-numbering scheme-(the thermal ellipsoids are drawn at the 30% probability level and H atoms are shown as small spheres of arbitrary radii) (a) and the theoretical geometric structure of the title compound (b).

RESULTS AND DISCUSSION

X-Ray Studies and Optimized Molecular Geometry

The single crystal X-ray analysis reveals that the molecule was located on a two-fold axis (Fig. 2a). It crystallizes in the monoclinic system (sp. gr. $P2_1/c$) with one molecule per the unit cell. Hydrogen-bond geometry is given in Table 2.

Each macrocycle use thiazole nitrogen (N1) and oxygen from the chloroacetic acid (O1) as hydrogen-bond acceptors, whereas the aromatic proton (H19) and hydrazide group (H15) act as donors [41]. The lattice stabilization is obtained through C–H···X (X = O, N) hydrogen bonds and π-ring stacking interactions. The X-ray crystal structure analysis revealed a string-

Table 2. Hydrogen-bond geometry (Å, deg) for the title compound

D–H···A, Å	D–H, Å	H···A, Å	D···A, Å	D–H···A, deg
C15–H15···N1	0.93	2.22	2.816(2)	121
C19–H19···O1[(i)]	0.93	2.53	3.275(3)	137
C1–H1···Cg4[(ii)]	0.93	2.86	3.755(2)	162

[i] Symmetry code: $-1 + x, y, -1 + z$.
[ii] Cg4 is a phenyl ring.

like arrangement of macrocyclic connected by intermolecular C–H···O hydrogen bonding (H19···O1 = 2.53 Å, C19–H19···O1 = 137°). This pattern was build up the lattice as shown in Fig. 3, this arrangement was held in place by C–H···O interactions. The intramolecular hydrogen bonding was between the thiazole nitrogen (N1) and the CH (H15) of the molecule (N1···H15 = 2.22 Å).

The optimized structure parameters of the NNP2CH calculated by DFT method and listed in Table 3 are in accordance with the atom numbering scheme given in Fig. 2a. As can be seen from Table 3, slight variations in the bond lengths and angles are observed because the molecular states are different during the experimental and theoretical processes. The agreement between the theoretical and experimental results (bond lenght and bond angles) has been expressed by obtained linear function formulas: $y = 1.0421x - 0.0459 R^2 = 0.9946$ (6-31G(*d*)), $y = 1.0445x - 0.0502$, $R^2 = 0.9947$ (6-311G+(*d*)) for bond lengths; $y = 1.0445x - 0.0502 R^2 = 0.9947$ (6-31G(*d*)), $y = 0.9737x + 2.5398 R^2 = 0.9708$ (6-31G(*d*)), $y = 0.9751x + 2.3621 R^2 = 0.9688$ (6-311G+(*d*)) for bond angles. The geometrical parameters for the title molecule are normal and consistent with those recently reported for thiazole derivative [42].

A logical method for globally comparing the structures obtained with the theoretical calculations is by superimposing the molecular skeleton with that obtained from X-ray diffraction, giving a root mean squared error (RMSE) of 0.830 Å for B3LYP/6-31G(*d*) and 0.857 Å for B3LYP/6-311G+(*d*). Figure 4 shows the atom-by-atom superimposition of the structures calculated (magenta) on the X-ray structure (mahogany) of the title compound.

IR Spectroscopy

Vibrational spectral measurements were made for *N*-[4-(3-methyl-3-phenyl-cyclobutyl)-thiazol-2-yl]-*N*'-pyridin-2-ylmethylene-chloro-acetic acid hydrazide. Optimized geometrical structure and harmonic vibrational frequencies were computed by DFT (B3LYP) methods using the same basis sets. Complete assignments of the observed spectra were suggested. The calculated vibrational frequencies (scaled) and approximate description of normal modes obtained using B3-base DFT methods are listed in Table 4. Gaussview program [43] was used to assign the calcu-

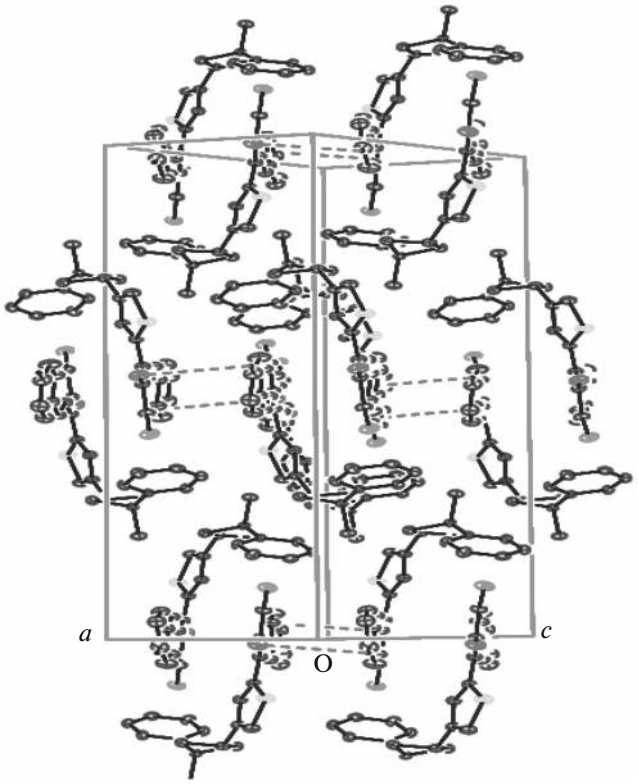

Fig. 3. Packing diagram of the title compound.

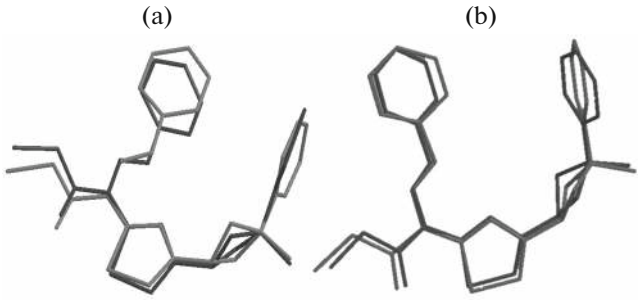

Fig. 4. Atom-by-atom superimposition of the structures calculated (magenta) and X-ray structure (mahogany) of the title compound (hydrogen atoms have been omitted for clarity) for B3LYP/6-31G(*d*) level (a) and B3LYP/6-311G+(*d*) level (b).

lated harmonic frequencies. The FT-IR spectrum of the title compound is shown in Fig. 5.

The FT-IR spectra have some characteristic bands of the stretching vibrations of the C–H, $C–H_2$, $C–H_3$, C–C, C–N, C=N, C–S, and C–Cl groups. The aromatic structure shows the presence of C–H stretching vibrations in the region 2900–3150 cm^{-1}, which is the characteristic region for the identification of the C–H stretching vibrations. In this region, the bands are not appreciably affected by the nature of the substituent [44]. The C–H aromatic stretching mode was observed at 3162 and 3100 cm^{-1} experimentally, and calculated at 3104–3080 cm^{-1} for 6-31G(*d*) and at (3092/3072)–3083 cm^{-1} for 6-311G+(*d*) basis sets. In the higher frequency region, almost all vibrations belong to symmetric and asymmetric νCH_2 and νCH_3 (in cyclobutane ring and chloroacetic acid group) stretching vibrations, respectively. The ranges of frequencies obtained by B3LYP method in this region are (2950/2947)–3009 cm^{-1} and (3011/3008)–3061 cm^{-1} for 6-31G(*d*) ($\nu_s CH_2$(B) and $\nu_{as} CH_2$(E)) and 2948–3015 cm^{-1} and 3012–3068 cm^{-1} for 6-311G+(*d*) levels ($\nu_s CH_2$(B) and $\nu_{as} CH_2$(E)), respectively. Bands at 2993–2986 cm^{-1} for 6-31G(*d*) and 2991 cm^{-1} for 6-311G+(*d*), and 2921 for 6-31G(*d*) and 2924 cm^{-1} for 6-311G+(*d*) correspond to the asymmetric and symmetric $C–H_3$ stretching modes, respectively. Vibrations characteristic to the thiazole ring were observed at 1580, 1534, and 628 cm^{-1} due to νC=N, νC–C, and νC–S, while that have been calculated at 1475, 1523, and 820 cm^{-1} for B3LYP/6-31G(*d*), and at 1464, 1571/1526, and 823 cm^{-1} for B3LYP/6-311+G(*d*) basis set. This bands were observed at 1580, 1534, and 738 cm^{-1} experimentally, and calculated at 1476, 1526, and 726 cm^{-1} (6-31G(*d*) basis set) for *N*'-benzylidene-*N*-[4-(3-methyl-3-phenylcyclobutyl)-thiazol-2-yl]-chloro-acetic acid hydrazide [42]. On the other hand, νC=O stretching and νC–Cl stretching bands were observed at 1716 and 781 cm^{-1}, that have been calculated using B3LYP method at 1733, 771 and 1722, 774 cm^{-1} for 6-31G(*d*) and 6-311G+(*d*) basis sets, respectively. These assignments are also supported by Demir et al. [42]. Other calculated vibrational frequencies can be seen in Table 4. The correlations between the experimental and calculated vibrational parameters are given in Fig. 6. According to our calculations, B3LYP method correlates well for the vibrational parameters.

Chemical Shifts of Nuclei of Carbon and Hydrogen Atoms

The chemical shifts of the relevant protons were given in Table 5 together with the values calculated theoretically (i) by our method of examining only the ring current effects [45] of the aromatic moieties in two series of compounds and (ii) by exclusive gauge

Table 3. Selected optimized and experimental geometry parameters of the title compound in ground state

Parameter	Experimental	Calculated	
		DFT/B3LYP 6-31G(*d*)	DFT/B3LYP 6-311G+(*d*)
Bond lengths, Å			
S1–C1	1.706(2)	1.737	1.735
S1–C3	1.727(2)	1.768	1.766
N1–C3	1.293(2)	1.302	1.300
N1–C2	1.377(2)	1.382	1.382
C2–C1	1.341(2)	1.364	1.362
C11–C22	1.765(2)	1.794	1.795
N3–C15	1.253(2)	1.285	1.282
N3–N2	1.393(3)	1.382	1.380
C3–N2	1.408(2)	1.414	1.416
N2–C21	1.382(2)	1.405	1.408
C6–C8	1.532(4)	1.540	1.539
C6–C5	1.540(3)	1.562	1.563
C6–C7	1.550(2)	1.563	1.563
C5–C4	1.544(2)	1.558	1.557
C16–N4	1.331(2)	1.346	1.343
N4–C20	1.341(3)	1.335	1.333
Bond angles, deg			
C1–S1–C3	88.11(8)	87.677	87.686
C3–N1–C2	110.44(14)	111.942	112.007
C15–N3–N2	121.94 (14)	123.485	124.177
N1–C3–S1	115.32 (13)	114.553	114.523
N2–C3–S1	122.36 (12)	122.490	122.392
C21–N2–N3	120.83(13)	112.971	112.909
C6–C5–C4	89.53(14)	89.411	89.181
C1–C2–N1	114.59(16)	114.211	114.113
C1–C2–C4	127.02(16)	126.590	125.870
C4–C7–C6	89.08(14)	89.375	89.182
O1–C21–C22	124.41(17)	123.683	123.779
N2–C21–C22	114.27(15)	114.939	114.868
N4–C16–C15	114.63(17)	113.496	113.997
N3–C15–C16	120.26(17)	119.734	119.311
C21–C22–Cl1	110.98(14)	111.162	111.183
C16–N4–C20	116.29(19)	117.938	118.138
Torsiyon angles, deg			
C11–C22–C21–O1	−3.7	0.141	−0.003
O1–C21–N2–C3	−4.8	−0.114	0.002
S1–C3–N2–N3	−156.8	−179.302	−179.992
C22–C21–N2–N3	−1.4	−0.220	0.000
C4–C5–C6–C7	−18.9	−17.330	−18.411

Table 4. Comparison of the observed and calculated vibrational spectra of the title compound

Assignments	Experimental	Calculated	
	IR with KBr, cm^{-1}	B3LYP 6-31G(*d*)	B3LYP 6-311G+(*d*)
νC–H(A)	3264	3141	3134
$\nu C_{15}–H_{15}$	3215	3121	3115
$\nu_s C–H(D)$	3162	3104	3092/3072
$\nu_{as} C–H(D)$	3132	3091/3072	3091/3072
$\nu_s C–H(C)$	3100	3080	3083
$\nu_{as} C–H(C)$	3080	3070/3062/3049	3072
$\nu_{as} C–H_2(E)$	3053	3061	3068
$\nu_{as} C–H_2(B)$	3020	3011/3008	3012
$\nu_s C–H_2(E)$	3010	3009	3015
$\nu_{as} C–H_3$	2954	2993–2986	2991
νC–H(B)	2928	2961	2966
$\nu_s C–H_2(B)$	2862	2950–2947	2948
$\nu_s C–H_3$	2577	2921	2924
νC=O	1716	1733	1722
$\nu C_{15}–N_3$	1714	1615	1610
νC=C(C)	1608	1600–1576	1594
νC–C(D)	1566	1574–1563	1560/1571
νC–C(A)	1534	1523	1571/1526
γC–H(C)	1493	1487/1434	1485
$\nu C_3=N_1$(A)	1580	1475	1464
$\alpha C–H_3$	1479	1462	1468
γC–H(D)	1464	1456/1422	1422
$\alpha C–H_2(B)$	1444	1442	1439
$\alpha C–H_2(E)$	1435	1413	1410
$\omega C–H_3$	1397	1375	1370
$\omega C–H_2(E) + \nu C_3=N_1 + \gamma C–H(D + F)$	1368	1292	1341
$\nu C_9–C_6$	1251	1282	1284/1282
$\nu C_3–N_2–N_3 + \gamma C–H(F) + \omega C–H_2(E)$	1240	1229–1205/1180–1175	1226–1202
$\omega C–H_2(B)$	1222	1203	1199
αC–H(C)	1203	1166	1166
$\delta C–H_2(E)$	1148	1152	1163
αC–H(D)	–	1136	1137
γC–H (A)	1125	1132	1136
$\delta C–H_2 + \gamma C–H(B)$	1093	1111/1029	1029
αC–H(D)	1078	1079	1081
Θ(A)	1021	1006/875	1009
Θ(C)	970	978	985
δ(D)	947	971/947	980
Θ(D)	990	970	978–976
δ(C)	1021	950/926	959
Θ(B)	923	932	936
β deformation (E)	897	909	910
νC–S (A)	628	820	823
νC–Cl	781	771	774
β deformation (C)	768	745	748/687
β deformation (A)	747	727/676	676
β(E)	738	710	773
ω(C)	704	687	748/687
β(D)	590	609–574	616
β deformation (E + F)	545	566/531	578

Vibrational modes: ν, stretching; s, symmetric; as, asymmetric; α, scissoring; γ, rocking; ω, wagging; δ, twisting; θ, ring breathing; β, in-plane bending. Abbreviations: A, thiazole ring; B, cyclobutane ring; C, phenyl ring; D, pyridin ring; E, chloro acetic acid group; F, hydrazit group.

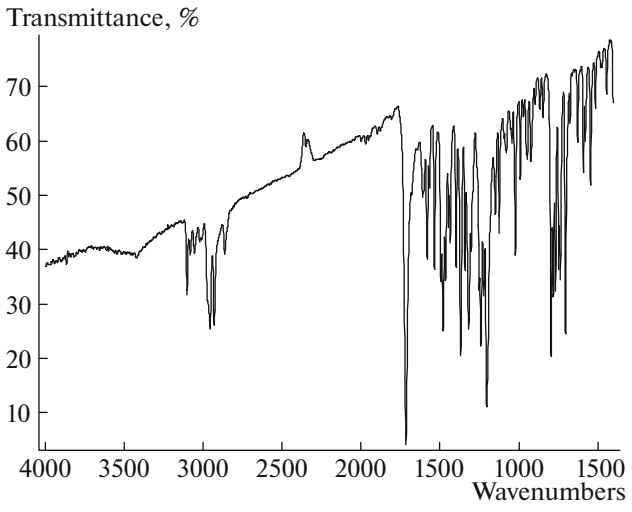

Fig. 5. The FT-IR spectrum of the title compound.

invariant atomic orbitals (GIAO) [46, 47] calculations. Comparison of the experimental and theoretically calculated chemical shift differences between the relevant protons (Table 5) demonstrates the excellent agreement in both direction (high- or low-field) and amount; thus, the ^{1}H and ^{13}C NMR spectra of corresponding compounds in two series are correctly described by the HF and DFT calculations. The NMR spectral data for NNP2CH were compiled in Table 5. These chemical shifts were calculated with the GIAO method [48] and 6-31G(*d*) and 6-311G+(*d*) basis sets. ^{1}H chemical shift values (with respect to TMS) were calculated and found to be 6.26–0.29 ppm at 6-31G(*d*) level and 6.79–0.02 ppm at 6-311G+(*d*), whereas the experimental results were observed to be 8.35–1.57 ppm. The ^{1}H NMR spectrum is indicated as evident from the appearance of a singlet for methyl protons at $\delta = 1.57$ ppm. The singlet is assigned to H8' (C8) atoms that have been calculated at 3.24 ppm (6-31G(*d*)) and 3.44 ppm (6-311G+(*d*,*p*)) for the B3LYP level. All carbon atoms give peaks at the range of 148.37–5.82 ppm for 6-31G(*d*) and 167.56–1.87 ppm for 6-311G+(*d*,*p*) level. The result shows that the range ^{13}C NMR chemical shift of the typical organic molecule is usually greater than 100 ppm [49, 50]; the accuracy ensures reliable interpretation of spectroscopic parameters. The chlor, oxygen and sulfur atoms that are present at three different positions in the molecule shows electronegative property, so that the chemical shift of C22, C21, C1, and C3 seems to be 43.15, 158.65, 114.27, and 167.57 ppm, respectively. As can be seen from Table 5, the theoretical ^{1}H and ^{13}C chemical shift values for the title compound are generally closer to the experimental ^{1}H and ^{13}C chemical shift data.

Molecular Electrostatic Potential

Molecular electrostatic potential (MEP) has proved itself as an effective tool for quantitatively assessing various non-covalent interactions, such as hydrogen-bonding, halogen bonding, and cation–π interactions [51–54]. Electrostatic properties of molecules can be computed approximately using discrete point charges located on the atomic sites at the van der Waals surface or at surfaces farther away from the molecules [55–59].

The quantitative analysis of $V(r)$ (electrostatic potential) initially consisted mainly of locating and identifying the most negative potentials, V_{min}, which

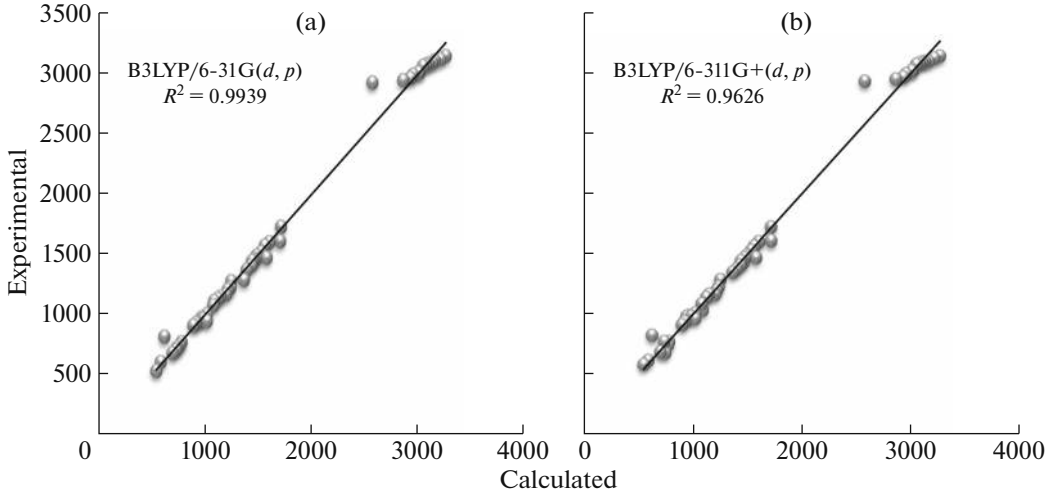

Fig. 6. Correlation graphics of calculated and experimental frequencies of the title compound for B3LYP/6-31G(*d*,*p*) level (a) and B3LYP/6-311G+(*d*,*p*) level (b).

Table 5. Theoretical and experimental ^{13}C and ^{1}H isotropic chemical shifts (with respect to TMS, all values in ppm) for the title compound

Atom	Experimental ($CDCl_3$)	Calculated	
		B3LYP/6-31G(*d*)	B3LYP/6-311G+(*d*)
C1	114.27	100.01	96.26
C2	152.71	144.85	149.11
C3	167.57	148.37	163.71
C4	30.94	17.79	5.59
C5	40.78	21.44	10.81
C6	38.93	29.78	15.44
C7	40.78	24.76	13.57
C8	29.93	5.82	1.87
C9	152.70	140.51	147.28
C10	124.72	107.97	113.26
C11	125.35	109.7	115.39
C12	128.21	104.85	108.70
C13	125.35	110.14	115.97
C14	124.72	108.25	113.47
C15	149.67	137.19	147.99
C16	151.92	142.12	148.22
C17	114.27	101.27	103.01
C18	136.66	117.24	127.45
C19	120.76	103.28	105.24
C20	147.92	135.31	143.31
C21	158.65	155.9	167.56
C22	43.15	36.63	27.45
H1	7.04	3.16	3.23
H4	3.84	0.29	0.02
H5*	2.61	0.76	1.51
H7*	2.65	1.09	1.51
H8*	1.57	3.24	3.44
H10	7.10	4.36	4.41
H11	7.20	4.48	4.67
H12	7.24	4.26	4.35
H13	7.30	4.57	4.75
H14	7.31	4.52	4.73
H15	8.35	6.26	6.79
H17	7.34	4.98	5.06
H18	7.38	4.9	5.33
H19	7.41	4.42	4.51
H20	7.78	6.17	6.42
H22*	4.84	1.38	1.00

***** Average.

were usually associated with: (a) the lone pairs of the more electronegative atoms, such as N, O, F, Cl, S and Br; and (b) unsaturated, aromatic and strained carbon-carbon bonds. These V_{min} could is often related to reactive properties, for instance, the pK_α values of azine nitrogens [60], and epoxide carcinogenicity [61]. More recently, attention has been focused on the electrostatic potential computed on the molecular "surface", and both positive and negative extrema, $V_{S,max}$ and $V_{S,min}$, have been used to establish quantitative relationships. For example, we have shown that, for a large variety of molecules, the $V_{S,max}$ and $V_{S,min}$ correlate with hydrogen bond acidity and basicity, respectively [62]. This overall approach has been useful, but it has been limited in scope; the V_{min}, $V_{S,min}$, and $V_{S,max}$ values are certainly key features of the molecular electrostatic potential, but they do not convey all the information that is contained in V(r).

The potential surface scan with the B3LYP/6-311G+(*d*) level of theoretical approximations has been performed for the title molecule (Fig. 7). The negative (red and yellow) regions of MEP were related to electrophilic reactivity and the positive (blue) ones to nucleophilic reactivity shown in Fig. 7a. As can be seen, this molecule has several possible sites for electrophilic attack. Negative regions were found in the studied molecule around the O1 atom of the carbonyl group, the S1 atom of thiazole ring, the N4 nitrogen atom of the pyridine ring. The negative V(r) values are −0.0562 a.u. for O1, which is the most negative region; −0.0562 a.u. for O1; −0.0264 a.u. for S1; −0.0333 a.u. for N4 atom, which is the least negative region. Thus, it would be predicted that an electrophile would preferentially attack the title molecule at the O1 and N4 positions. Furthermore, we found a maximum value of +0.032 a.u. on the C19–H19 bond on the positive regions of V(r), indicating that this site is probably involved in nucleophilic processes.

The lines are drawn in the contour map clearly show the flow of the electron density in title molecule (Fig. 7b). The red color dominating area, where the nitrogen and oxygen atoms were located, is found to be highly negative, and other colored parts signify the positive region of the molecule. Additionally, the total electron density is mapped to the electrostatic potential surface; the isosurface representation of the total electrostatic potential of the title compound is shown in Fig. 7c.

Mulliken Population Analysis

The calculation of effective atomic charges plays an important role in the application of quantum mechanical calculations to molecular systems. The charge distribution on different atoms (C, N, O, S, and Cl) for NNP2CH from Mulliken population analysis (MPA) procedures using B3LYP method is listed in Table 6.

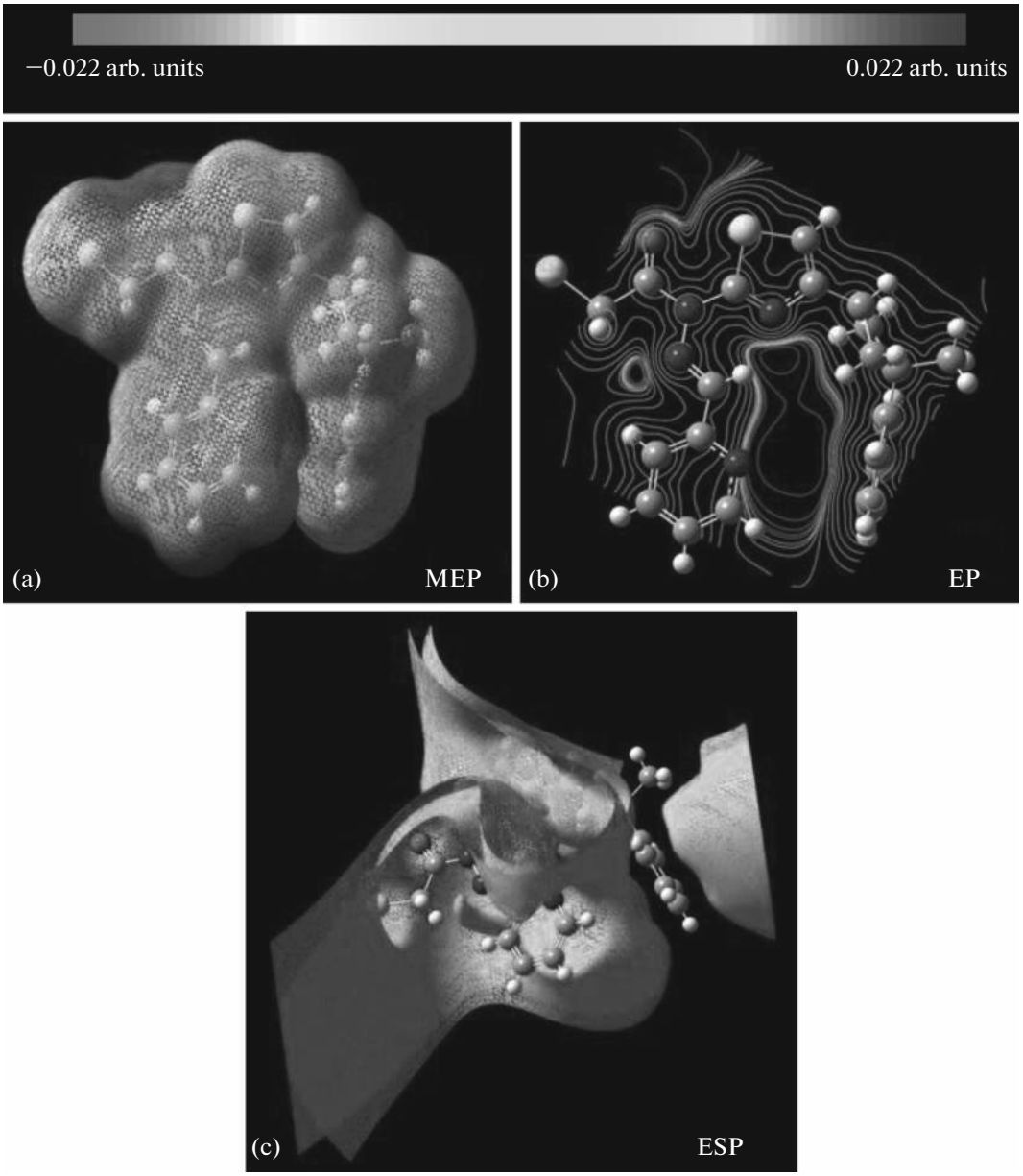

Fig. 7. Molecular electrostatic potential map calculated at B3LYP/6-311G+(*d*) level (a), the contour map of molecular electrostatic potential surface of the title compound (b), and the isosurface representation of total electrostatic potential of the title compound (c).

Graphical representations of atomic charges and natural charges on the atom are shown in Fig. 8.

Molecular Orbitals

The frontier orbitals of a chemical species, highest occupied molecular orbital (HOMO) and lowest unoccupied molecular orbital (LUMO), are quite important for the determination of their reactivity. Fukui et al. [63] were first who recognized this. The E_{HOMO} is often associated with the electron donating ability of the molecules. The E_{HOMO} indicates the molecular ability in donating electrons to appropriate acceptor molecules with low energy empty molecular orbital. E_{LUMO} indicates the ability of the molecule to accept electrons. The lower value of E_{LUMO}, the more probable it is that the molecule would accept electrons. Consequently, concerning the value of the energy gap $\Delta E = E_{LUMO} - E_{HOMO}$, higher values of ΔE will provide lower reactivity to a chemical species.

Table 6. Mulliken charges of *N*-[4-(3-methyl-3-phenyl-cyclobutyl)-thiazol-2-yl]-*N*'-pyridin-2-ylmethylene-chloro-acetic acid hydrazide with 6-31G(*d*) and 6-311+G(*d*)

Atoms	Mulliken charge 6-31G(*d*)	Atoms	Mulliken charge 6-311G+(*d*)	Atoms	Mulliken charge 6-31G(*d*)	Atoms	Mulliken charge 6-311G+(*d*)
Cl1	−0.039	Cl1	0.344	H1	0.174	H1	0.247
O1	−0.442	O1	−0.131	H4	0.130	H4	0.212
S1	0.320	S1	0.054	H5*A*	0.137	H5*A*	0.245
N1	−0.524	N1	0.010	H5*B*	0.162	H5*B*	0.260
N2	−0.363	N2	−0.016	H7*A*	0.137	H7*A*	0.246
N3	−0.315	N3	0.343	H7*B*	0.161	H7*B*	0.262
N4	−0.469	N4	0.132	H8*A*	0.140	H8*A*	0.247
C1	−0.431	C1	−0.328	H8*B*	0.149	H8*B*	0.253
C2	0.366	C2	0.481	H8*C*	0.149	H8*C*	0.253
C3	0.306	C3	0.235	H10	0.125	H10	0.216
C4	−0.174	C4	−0.079	H11	0.125	H11	0.205
C5	−0.291	C5	−1.351	H12	0.122	H12	0.200
C6	0.016	C6	1.459	H13	0.125	H13	0.204
C7	−0.289	C7	−1.355	H14	0.125	H14	0.217
C8	−0.452	C8	−1.236	H15	0.232	H15	0.339
C9	0.147	C9	1.647	H17	0.152	H17	0.233
C10	−0.177	C10	−0.694	H18	0.149	H18	0.234
C11	−0.127	C11	−0.460	H19	0.144	H19	0.227
C12	−0.133	C12	−0.423	H20	0.151	H20	0.222
C13	−0.127	C13	−0.458	H22*A*	0.228	H22*A*	0.305
C14	−0.177	C14	−0.677	H22*B*	0.228	H22*B*	0.306
C15	0.045	C15	−0.597				
C16	0.276	C16	−0.322				
C17	−0.151	C17	0.947				
C18	−0.105	C18	−1.409				
C19	−0.138	C19	−0.089				
C20	0.041	C20	−0.169				
C21	0.616	C21	0.093				
C22	−0.454	C22	−1.084				

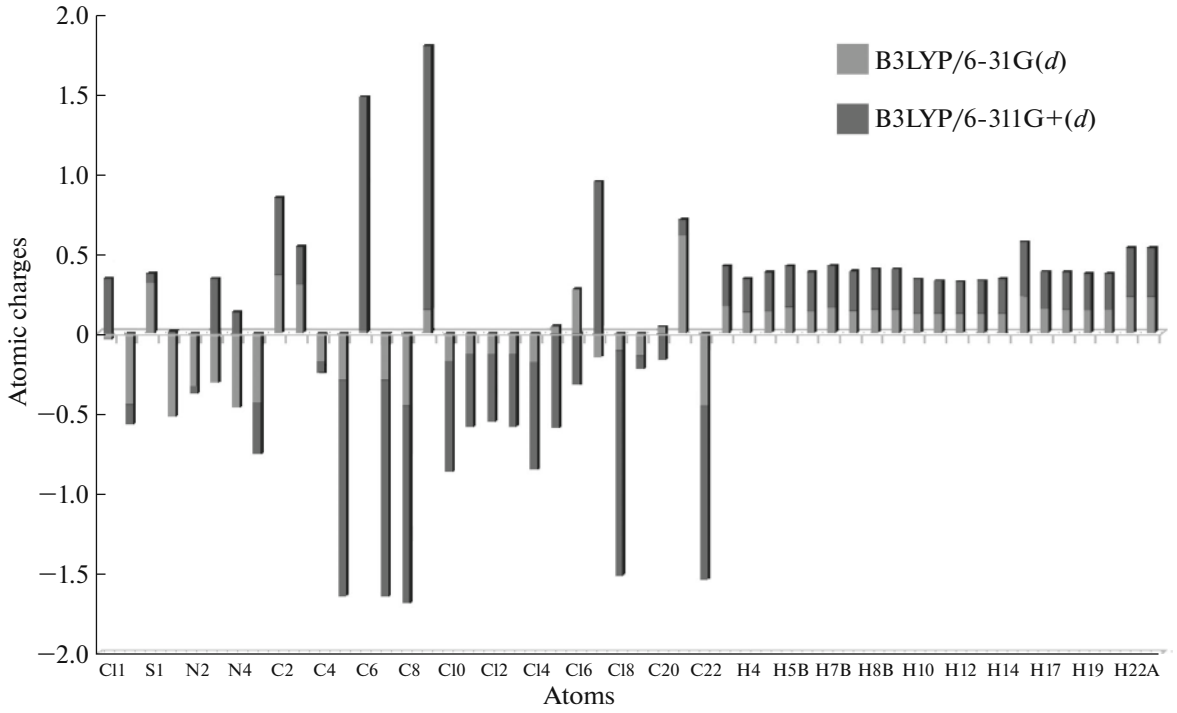

Fig. 8. Comparison of different basis sets for calculated atomic charges of the title compound.

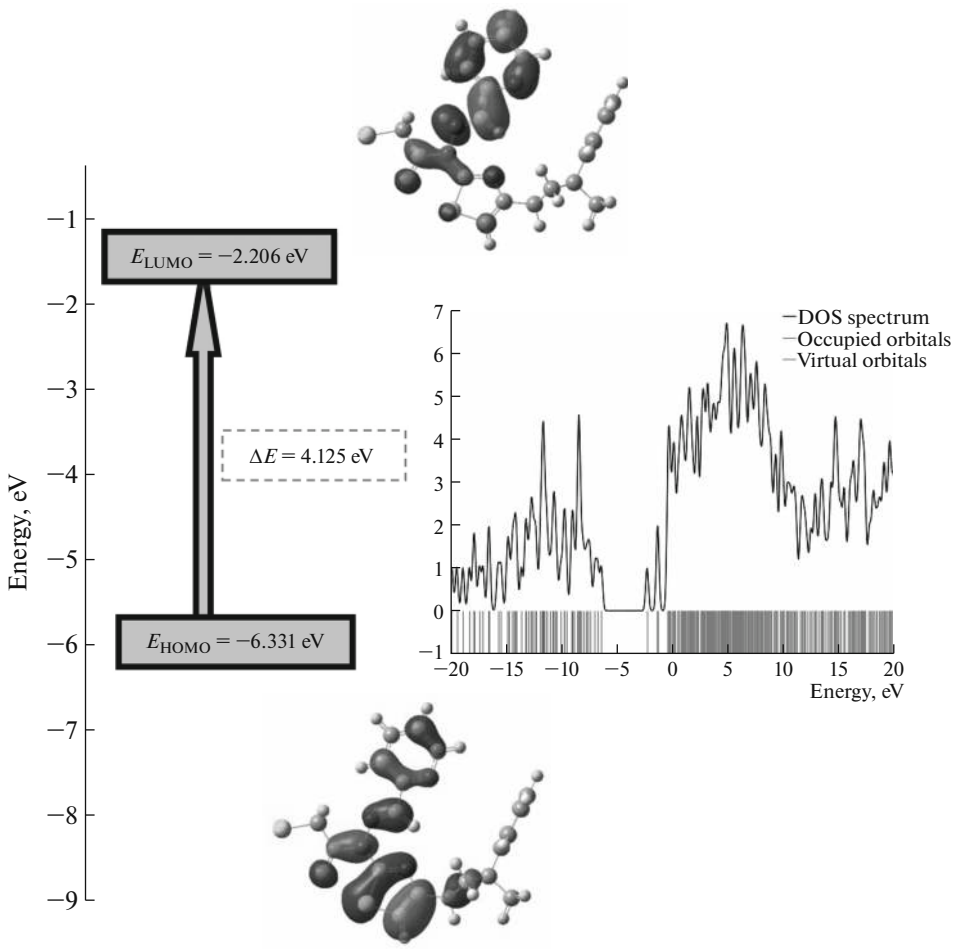

Fig. 9. Molecular orbital surfaces and energy levels given in boxes for the HOMO, LUMO and calculated the total electronic density of states diagram of the title compound computed at B3LYP/6-311G+(*d*) level.

Table 7. HOMO–LUMO energy calculated by B3LYP with 6-31G(*d*) and 6-311G+(*d*) methods

Parameters	B3LYP/6-31G(*d*)	B3LYP/6-311G+(*d*)
HOMO, eV	–6.036	–6.331
LUMO, eV	–1.858	–2.206
ΔE, eV	4.178	4.125
HOMO–1, eV	–6.361	–6.657
HOMO–2, eV	–6.603	–6.910
LUMO+1, eV	–0.941	–1.276
LUMO+2, eV	–0.782	–1.238
Total energies, a.u.	–2003.547	–2003.863

Lower values of the energy difference will indicate the higher reactivity of the molecules because the energy to remove an electron from the last occupied orbital to the first unoccupied orbital will be low [64, 65].

A visual inspection of the molecular orbitals, as shown in Fig. 9 for the title compound, explains this observation. Thus, while the LUMO orbitals reside exclusively in the thiazole, furan, cyclobutane ring and hydrazide group, we have localization of the HOMO on the furan, thiazole ring and hydrazide group. HOMO and LUMO energies, calculated by B3LYP/6-31G(*d*) and 6-311G+(*d*), are listed in Table 7. Besides, Gauss-Sum 3.0 Program [66] was used to calculate group contributions to the molecular orbitals (HOMO and LUMO) and prepare the density of the state (DOS), as shown in Fig. 9. The DOS plot provides a diagrammatic view of the molecular orbital contributions, computed by the GaussSum 3.0 program [65] at B3LYP/6-311G+(*d*).

CONCLUSION

In the present work, a complete X-ray analysis has been made for proper diffraction results of *N*-[4-(3-methyl-3-phenyl-cyclobutyl)-thiazol-2-yl]-*N'*-pyridin-2-ylmethylene-chloro-acetic acid hydrazide. A complete vibrational and molecular structure analysis has been performed based on the quantum mechanical approach to DFT calculation using B3LYP/6-31G(*d*) and B3LYP/6-311G+(*d*) basis sets. Chemical shifts of nuclei of carbon and hydrogen atoms, and the vibrational frequencies of the fundamental modes of the title compound have been precisely assigned and analyzed, and the theoretical results have been compared with the experimental vibrations. The intermolecular charge transfer is evidenced by Mulliken charge population analysis. HOMO and LUMO energy gap reveal that the energy gap reflects the chemical activity of the molecule. To predict the reactive sites for electrophilic and nucleophilic attack for the NNP2CH molecule, the MEP at the B3LYP/6-311G+(*d*) optimized geometry was calculated.

REFERENCES

1. J. R. Hill, L. Subramanian, and A. Maiti, *Molecular Modeling Techniques in Materials Science* (Taylor and Francis/CRC, Boca Raton, FL, 2005).
2. J. B. Foresman and A. E. Frisch, *Exploring Chemistry with Electronic Structure Methods* (Gaussian, Pittsburgh, PA, 1996).
3. N. Agarwal, S. Kumar, A. K. Srivastava, and K. P. C. Sarkar, Ind. J. Het. Chem. **6**, 291 (1997).
4. R. C. Sup, R. Y. Sukp, and C. W. Bang, Korean J. Med. Chem. **5**, 72 (1995).
5. S. I. Sumistov and Z. A. Bofoshko, USSR Patent No. 154861 (1964).
6. J. D. Hadjipavlou-Litina and A. Geronikaki, Arz. Forsch. Drug Res. **46**, 805 (1996).
7. L. D. Hadjipavlou, A. Geronikaki, and E. Sotiropoulou, Res. Commun. Chem. Pathol. **79**, 355 (1993).
8. A. Geronikaki, D. Hadjipavlou-Litina, and M. Amourgianou, Il Farmaco **58**, 489 (2003).
9. M. Tsuruoka and I. Seikutsugaka, Med. Biol. **10**, 296 (1947).
10. J. R. Merchant, G. Martysen, and N. S. Venkatesh, Indian J. Chem. B **20**, 493 (1981).
11. G. Maass, U. Immendoerfer, B. Koenig, et al., Antimicrob. Agents Chemother. **37**, 2612 (1993).
12. M. P. Anna, G. Athina, M. Remi, et al., Bioorg. Med. Chem. **11**, 2983 (2003).
13. R. P. Kapoor, M. K. Rastogi, R. Khanna, et al., Indian J. Chem. B **23**, 390 (1984).
14. J. V. Metzger, in *Comprehensive Heterocyclic Chemistry*, (Pergamon, Oxford, 1984), p. 235.
15. B. Dash, M. Patra, and S. Praharaj, Indian J. Chem. B **19**, 1378 (1980).
16. J. Michel Grivy, F. Tellez, S. Bernes, et al., Inorg. Chim. Acta **339**, 532 (2002).
17. A. Benalte-Garcia, F. J. Garcia-Barros, F. J. Higes-Rolando, et al., Polyhedron **18**, 2907 (1999).
18. K. Lemma, J. Berglund, N. Farrell, et al., J. Biol. Inorg. Chem. **5**, 300 (2000).
19. M. J. M. Campbell, Coord. Chem. Rev. **15**, 279 (1975).
20. S. Padhye and G. B. Kauffman, Coord. Chem. Rev. **63**, 127 (1985).
21. S. Bhattcharya and M. Thomas, Tetrahedron Lett. **41**, 10313 (2000).
22. B. Imperiali, J. Org. Chem. **63**, 6727 (1988).
23. D. Parker, S. P. White, and M. Brookhart, Chem. Commun. **1**, 47 (2000).
24. A. Torrado, G. K. Walkup, and B. Imperiali, J. Am. Chem. Soc. **120**, 609 (1988).
25. R. B. Thompson, Z. Ge, M. Patchan, et al., Bioelectronics **11**, 557 (1996).
26. J. Sitkowski, L. Stefaniak, T. Dziembowska, et al., J. Mol. Struct. **381**, 177 (1996).
27. R. Castro, J. A. Garcia-Vazquez, J. Romero, et al., Polyhedron **12**, 2241 (1993).

28. S. Saydam, Synth. React. Inorg. Met. Org. Chem. **32**, 437 (2002).
29. H. Ieda, H. Fujiwara, and Y. Fuchita, Inorg. Chim. Acta **319**, 203 (2001).
30. E. Borras, G. Alzuet, J. Borras, et al., Polyhedron **19**, 1859 (2000).
31. S. Saydam and C. Alkan, Pol. J. Chem. **75,** 29 (2001).
32. M. James, H. Kawaguchi, and K. Tatsumi, Polyhedron **16,** 1873 (1996).
33. G. Mohamed, Spectrochim. Acta, Part A **57,** 411 (2001).
34. R. G. Parr and W. Yang, *Density Functional Theory of Atoms and Molecules* (Oxford University Press, New York, 1989).
35. Stoe and Cie, *X-AREA Version 1.18 and X-RED32 Version 1.04* (Stoe and Cie, Darmstadt, Germany, 2002).
36. G. M. Sheldrick, *SHLEXS-97. Program for Refinement of Crystal Structures* (University of Göttingen, Germany, 1997).
37. L. J. Farrugia, J. Appl. Crystllogr. **30**, 565 (1997).
38. J. B. Foresman and A. Frisch, *Exploring Chemistry with Electronic Structure Methods* (Gaussian, Pittsburg, 1996).
39. J. P. Merrick, D. Moran, and L. Radom, J. Phys. Chem. A **111**, 11683 (2007).
40. R. Dennington, T. Keith, J. Millam, et al., *GaussView Version 3.07* (Semichem, Shawnee Mission, KS, 2003).
41. V. Haridas, S. Sahu, and P. Venugopalan, Tetrahedron **67**, 727 (2011).
42. S. Demir, M. Dincer, A. Cukurovali, et al., Int. J. Quantum Chem. **112**, 1016 (2012).
43. M. J. Frisch, G. W. Trucks, and H. B. Schlegel, *Gaussian 03 Revision C.02* (Gaussian, Pittsburgh, PA, 2003).
44. A. Teimouri, M. Emami, A.N. Chermahini, et al., Spectrochim. Acta Part A **71**, 1749 (2009).
45. S. Klod and E. Kleinpeter, J. Chem. Soc. Perkin Trans. **2**, 1893 (2002).
46. J. R. Ditchfield, Mol. Phys. **27**, 789 (1974).
47. J. P. Cheeseman, G. W.Trucks, T. A. Keith, et al., J. Chem. Phys. **104**, 5497 (1996).
48. K. Wolinski, J. F. Hilton, and P. Pulay, J. Am. Chem. Soc. **112**, 8251 (1990).
49. H. O. Kalinowski, S. Berger, and S. Braun, *Carbon-13 NMR Spectroscopy* (Wiley, Chichester, 1988).
50. K. Pihlaja, E. Kleinpeter (Eds.), *Carbon-13 Chemical Shifts in Structural and Sterochemical Analysis,* Ed. by K. Pihlaja and E. Kleinpeter (VCH, Deerfield Beach, 1994).
51. J. W. Zou, Y. J. Jiang, M. Guo, et al., Chem. Eur. J. **11**, 740 (2005).
52. H. Hagelin, T. Brinck, M. Berthelot, et al., Can. J. Chem. **73**, 483 (1995).
53. O. Lukin and J. Leszczynski, J. Phys. Chem. A **106,** 6775 (2002).
54. L. Joubert and P. L. A. Popelier, Phys. Chem. Chem. Phys. **4**, 4353 (2002).
55. P. C. Mishra and A. Kumar, Top. Curr. Chem. **174**, 27 (1995).
56. C. A. Reynolds, J. W. Essex, and W. G. Richards, J. Am. Chem. Soc. **114**, 9075 (1992).
57. J. Meister and W. H. E. Schwartz, J. Phys. Chem. **98**, 8245 (1994).
58. C. G. Mohan, A. Kumar, and P. C. Mishra, J. Mol. Struct. Theochem. **332**, 171 (1995).
59. R. Bonaccorsi, A. Pullman, E. Scrocco, et al., Theor. Chim. Acta (Berlin) **24**, 51 (1972).
60. P. Politzer and J. S. Murray, *Reviews in Computational Chemistry,* Ed. by K. B. Lipkowitz and D. B. Boyd (VCH, New York, 1991).
61. P. Politzer, P. R. Laurence, and K. Jayasuriya, Env. Health Persp. **61**, 191 (1985).
62. H. Hagelin. T. Brinck, M. Berthelot, et al., Can. J. Chem. **73**, 483 (1995).
63. K. Fukui, T. Yonezawa, and H. Shingu, J. Chem. Phys. **20**, 722 (1952).
64. N. Khalil, Electrochim. Acta **48**, 2635 (2003).
65. I. Lukovits, K. Palfi, I. Bako, et al., Corrosion **53**, 915 (1997).
66. N. M. O'Boyle, A. L. Tenderholt, and K. M. Langer, J. Comput. Chem. **29**, 839 (2008).